# Theoretical issues in tokamak confinement: (i) internal/edge transport barriers and (ii) runaway avalanche confinement

J. W. CONNOR 1), P. HELANDER 1), A. THYAGARAJA 1), F. ANDERSSON 2), T. FÜLÖP 2), L. -G. ERIKSSON 3), M. ROMANELLI 4)

1) EURATOM/UKAEA Fusion Association, Culham Science Centre, Abingdon, UK
2) Association EURATOM/NFR, Dept of Electromagnetics, Chalmers University of Technology, Göteborg, Sweden
3) Association EURATOM-CEA sur la Fusion, CEA Cadarache, France
4) ENEA, Centro Ricerche Energia FRASCATI, Via Enrico Fermi, Frascati (RM), Italy

e-mail contact of main author: jack.connor@ukaea.org.uk

**Abstract.** This paper summarises a number of distinct, but related, pieces of work on key confinement issues for tokamaks, in particular the formation of internal and edge transport barriers, both within turbulent and neoclassical models, and radial diffusion of avalanching runaway electrons. First-principle simulations of tokamak turbulence and transport using the two-fluid, electromagnetic, global code CUTIE are described. The code has demonstrated the spontaneous formation of internal transport barriers near mode rational surfaces, in qualitative agreement with observations on JET and RTP. The theory of neoclassical transport in an impure, toroidal plasma has been extended to allow for steeper pressure and temperature gradients than are usually considered, and is then found to become nonlinear under conditions typical of the tokamak edge. For instance, the particle flux is found to be a nonmonotonic function of the gradients, thus allowing for a bifurcation in the ion particle flux. Finally, it is shown that radial diffusion caused by magnetic fluctuations can effectively suppress avalanches of runaway electrons if the fluctuation amplitude exceeds $\delta B/B \sim 10^{-3}$.

## 1. Introduction

Transport processes control the confinement of plasma species. Often it is desirable that the transport should be as low as possible to improve tokamak performance. Of particular interest are the conditions for the creation of transport barriers: both internal ones (ITBs) and the edge ones associated with the L-H transition. In Section 2 we describe global computer simulations of tokamak transport that lead naturally to ITB formation. In H-mode a region of steep edge gradients is produced; in Section 3 we revisit neoclassical theory in these circumstances, showing how it predicts bifurcated particle fluxes, which perhaps could trigger the transition itself. However, on occasion substantial transport can be beneficial and in Section 4 we determine the lower limit on magnetic turbulence to prevent the formation of potentially damaging avalanches of runaway electrons in large tokamaks.

## 2. Computational studies of internal transport barriers (ITBs) using CUTIE

Recent tokamak confinement experiments (see, e.g., the review by Bell *et al* [1]) have exhibited the spontaneous formation of ITBs. The study of such structures is believed to be of considerable importance to fusion plasma physics, since they may offer routes to enhanced confinement regimes. Both neutral beam-heated (eg. JET [2]) and ECH

heated (eg. RTP [3]) discharges exhibit transport barriers. Results obtained using a computational approach to the study of ITBs (with special reference to JET [2]) based on the CUTIE code help one to understand their nature and the conditions for their formation.

The transport barriers are modelled by global (ie, 'whole tokamak', as opposed to 'flux tube'), nonlinear, electromagnetic, two-fluid simulations using CUTIE. CUTIE self-consistently calculates turbulence-driven flows in the large aspect ratio approximation. The equations of motion (given in full in Ref [4]) are obtained using quasi-neutrality, electron continuity, ion and electron momentum and energy balances, and Maxwell's equations. For simplicity, the equilibrium magnetic surfaces are taken to be circular, neglecting the Shafranov shift. Fourier analysis of the variables solved (electron density, the two temperatures, ion parallel velocity, the electrostatic potential, the potential vorticity and the poloidal magnetic flux function) with respect to the poloidal angle $\theta$ and the toroidal angle $\zeta$, leads to coupled nonlinear partial differential equations for the 'equilibrium profile' components independent of angle and the 'fluctuations' which do depend on the angular variables. The former are directly driven by the imposed sources of particles, energy (ohmic and auxiliary heating), current etc. Their gradients in turn drive instabilities which create the fluctuations and these can react back on the evolution of the equilibrium quantities through the medium of turbulent fluxes, over and above the basic neoclassical ones. The equations include, within the two-fluid model, physical effects such as visco-resistive tearing, ballooning, drift-Alfvén and ITG modes.

A key feature of the code is the simultaneous or 'co-evolution' of the turbulence and the equilibrium quantities. It turns out that the turbulent fluxes, although averaged over angles, are relatively rapidly varying functions of the radius and time. This feature is characteristic of 'mesoscale' turbulence: namely the space and time scales associated with it are intermediate between the system size and the ion Larmor radius, and confinement time and the shear Alfvén time, respectively. Such relatively rapid variations imply 'corrugations' in the equilibrium profiles. These are regions of relatively high local radial gradients and curvature in the radial profile quantities, which evolve rapidly compared with the confinement time. Internal transport barriers (ITBs) are special cases of such localized regions of high radial gradients, when they occur in the temperature or the density profiles, associated with relatively slow time-evolution.

In general, in our simulations, we find the low mode number part of the fluctuation spectrum is excited through an inverse cascade, even if one starts with high mode numbers. These relatively long wavelength modes are associated with low order rational values of the safety factor, $q$, and play a key role in the tendency of the system to 'self-organize' [5], by spontaneously forming structures like ITBs. Firstly, they generate fine-scale, intermittent turbulence through nonlinear and toroidal mode couplings and secondary instabilities (direct cascade). Secondly, they imply corrugated fluxes due to fast radial variation in amplitude, and nonlinear, dissipative, cross-phase relations. These fluxes react on profiles and determine the local gradients of both magnetic and electric fields, which in turn, drive/damp the turbulence in a relaxation process. In general, *two feed-back loops* have been identified, associated with the radial electric field, $E_{r0}(r,t)$, and the plasma current density, $j_0(r,t)$, respectively. The resulting nonlinear dynamics involves complex mode rotation, current filaments, internal mode-locking, relaxation oscillations, avalanches, and intermittent bursts of high $k,\omega$ turbulence.

To illustrate how this dynamic process works, we present the 'equilibrium' poloidal mag-

netic field, poloidal fluid velocity and the radial electric field evolution equations [4]:

$$\frac{\partial B_{\theta 0}}{\partial t} = \frac{\partial}{\partial r}\left[\frac{c^2\eta_{\rm nc}}{4\pi}\left(\frac{1}{r}\frac{\partial r B_{\theta 0}}{\partial r} - \frac{4\pi}{c} j_{\rm bs}\right)\right] \quad (1)$$

$$\frac{\partial v_{\theta 0}}{\partial t} = -\nu_{\rm nc}(v_{\theta 0} - v_{\theta {\rm nc}}) - \frac{1}{r}\frac{\partial}{\partial r}(r < \delta v_r^E \delta v_\theta^E >) + < \frac{\delta j_{||} \delta B_r}{m_i n_0 c} > \quad (2)$$

$$E_{r0} = \frac{1}{e n_0} p_{i0}' + \frac{(v_{\zeta 0} B_{\theta 0} - v_{\theta 0} B_{\zeta 0})}{c} \quad (3)$$

Note that the poloidal magnetic field evolution is influenced both by neoclassical resistivity $\eta_{\rm nc}$(itself a complicated function of temperature, $q$ etc), and more importantly, by $j_{\rm bs}$, the bootstrap current. Since the latter depends strongly on gradients, the evolution of $q$ is influenced by the turbulence through it. In principle, there ought to be other 'turbulence-driven' dynamo terms in Eq (1). Their effect is presently being studied and will be reported elsewhere. Equation(2) describes, within certain approximations, the dynamics of $v_{\theta 0}(r,t)$, the 'poloidal' fluid flow. This is driven by radial turbulent advection of poloidal momentum (also called the 'Reynolds stress') and the turbulent $\mathbf{j}\times\mathbf{B}$ force in the poloidal direction, averaged with respect to angles. The flows are damped by neoclassical effects: where $\nu_{\rm nc} = 0.67\epsilon^{-1}\tau_i^{-1}$ and $v_{\theta {\rm nc}} = -1.17(1-1.46\epsilon^{1/2})(cT_{i0}'/eB)$, with $\epsilon = r/R$ [6]. Thus the radial electric field, $E_{r0}(r,t)$, given by Eq (3), can acquire 'corrugations' both from such features in the ion pressure profile and the toroidal velocity. The latter must also be calculated in principle from a suitable momentum balance equation involving external sources and turbulent and neoclassical viscous damping. In present simulations, we simply assume that the toroidal flow is specified in terms of the Mach number and use the above equations to calculate $v_{\theta 0}$ and $E_{r0}$.

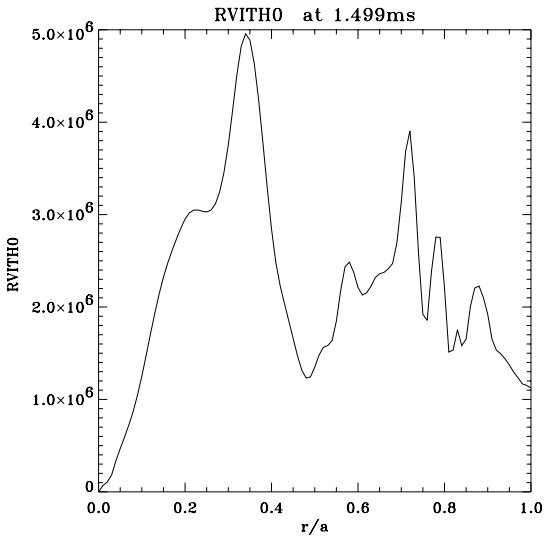


Figure 1: *Calculated $-cE_{r0}/B$ profiles (cm/s).*

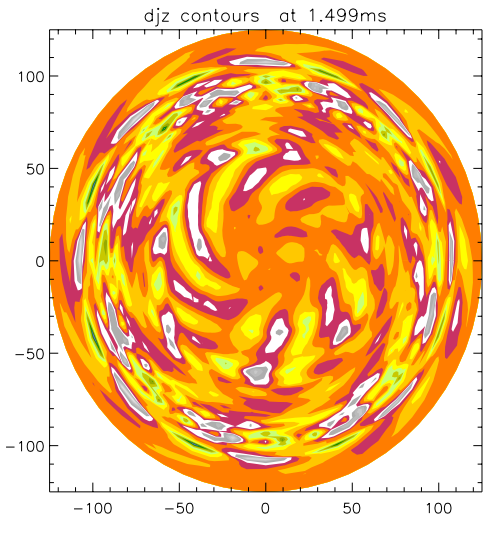


Figure 2: *Current fluctuations.*

In Figs 1-3 we show some typical results obtained using CUTIE, obtained from a high resolution ($100\times 64\times 32$ in $r,\theta,\zeta$ respectively) simulation of a JET-like shot (based on #49006: $P_{aux}\simeq 15$MW, $I_p\simeq 2.3$MA, $\bar{n}\simeq 1.5\times 10^{19}$ m$^{-3}$, $q_0\simeq 2.2$; toroidal Mach number $\simeq 0.3$). Figure 1 presents the calculated $E\times B$ flow profile after 1.5 ms of evolution from

simple Gaussian initial temperature and density profiles. The solution takes into account Eq (3) among others. It clearly shows highly 'corrugated', mesoscale sheared regions with strong 'jet-like' features. These influence the stability of the turbulence in their immediate vicinity. Figure 2 illustrates an instantaneous snap-shot of the computed current density fluctuations, revealing current filaments, 'streamers' (m=7 and higher harmonics, associated with the broad jet around $r/a \simeq 0.4$) and ballooning micro-turbulence involving an 8/3 resonance, close to the regions of strongly sheared $E \times B$ flow($r/a \simeq 0.8$). Movies made of the simulations reveal quite complex dynamical features associated with the rotation/evolution of the turbulent current filaments. Additional information relating to other quantities of interest such as the turbulent velocities can be found in Ref [4]. Figure 3a shows the calculated ion temperature profile at the same time as Figs 1 and 2. The barriers at $r/a \simeq 0.6$ and 0.8 are rather clear. The former is associated with a relatively small jet (Fig 1) whilst the latter with a more prominent one further out. The broad jet near $r/a \simeq 0.3$ is associated with a weaker barrier. Qualitatively the code captures barrier features in the experimental profile (obtained using charge exchange spectroscopy) shown in Fig 3b. The theoretical and experimental uncertainties preclude using the code as a predictive tool at present; its value is in indicating qualitatively how the turbulence and equilibrium interact and can evolve to generate transport barriers.
Detailed studies [4] have also been made of the RTP experiment [3], and results suggest that the model captures the main features of the observed barrier phenomena (role of rational surfaces, current filamentation, $E \times B$ flow-shear effects), at least qualitatively.

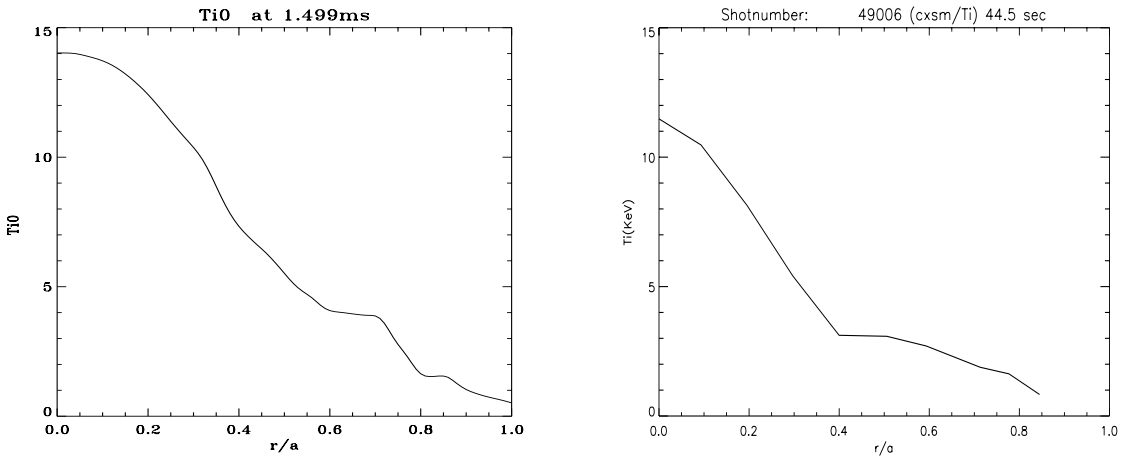


*(a)* *(b)*

Figure 3: *Calculated (a), and experimental (b) $T_i$ (keV) profiles (JET #49006)*

## 3. Nonlinear neoclassical transport in steep plasma edge profiles

In the H-mode pedestal region near the tokamak edge, the density and temperature profiles are frequently observed to be too steep for conventional neoclassical theory to be valid. The essential difficulty lies in the use of the expansion parameter $\delta \equiv \rho_\theta / L_\perp$, where $\rho_\theta$ is the poloidal ion gyroradius and $L_\perp$ the radial scale length of the density and temperature profiles. Neoclassical theory requires $\delta \ll 1$, and it is fundamentally difficult to construct a tractable transport theory when $\delta = O(1)$ since the plasma is then not in local thermodynamic equilibrium. When $\delta$ is infinitesimally small all plasma parameters are approximately constant on flux surfaces, but when $\delta$ is made larger poloidal asymmetries

become possible. Typically the first plasma parameter to develop a poloidal variation is the density, $n_z(\theta)$, of highly charged impurity ions [7], whose poloidal modulation is $\tilde{n}_z/n_z \sim \Delta \equiv \delta\hat{\nu}_{ii}z^2$, where $\hat{\nu}_{ii} \equiv L_\parallel/\lambda_{ii}$ is the collisionality, with $\lambda_{ii}$ the mean-free path for the bulk ions and $L_\parallel$ the connection length. In the tokamak edge, $\Delta$ can easily be of order unity while $\delta$ remains small, $\delta \ll 1$, $\Delta = O(1)$. In the present work we adopt this ordering [7,8,9], which is less restrictive than conventional neoclassical theory (which assumes $\Delta \ll 1$), thus enabling a non-uniform distribution of impurities over each flux surface. For simplicity, we restrict our attention to the case of a hydrogen plasma with a single species of highly charged ($z \gg 1$) impurity ions of appreciable density, $Z_{\rm eff} - 1 = n_z z^2/n_i = O(1)$. The electrons ($e$) and H ions ($i$) are taken to be collisionless while the impurities are assumed to be collisional. We also allow for toroidal plasma rotation to produce a poloidal impurity density asymmetry. The impurity Mach number is taken to be of order unity, $M_z^2 = m_z\omega^2R^2/2T_i = O(1)$, where $\omega$ denotes the angular rotation frequency, so that the main (H) ion Mach number is small, $M_i^2 = (m_i/m_z)M_z^2 \ll 1$.

The bulk-ion distribution function is obtained by solving the drift-kinetic equation in the banana regime in a conventional way, and is then used to calculate the friction force on the impurities in the parallel impurity momentum equation. When combined with the continuity equation and the requirement of quasineutrality, this gives the following equation for the normalised impurity density $n = n_z/\langle n_z\rangle$ [9],

$$(1+\alpha n)\frac{\partial n}{\partial \vartheta} = g\left(n - b^2 + \gamma\left(n - \left\langle nb^2\right\rangle\right)b^2\right) + \frac{\partial M^2}{\partial\vartheta}n - \left\langle n\frac{\partial M^2}{\partial\vartheta}\right\rangle b^2, \qquad (4)$$

where $\alpha \equiv \langle Z_{\rm eff}-1\rangle T_e/(T_e+T_i)$, $b \equiv B/\langle B^2\rangle^{1/2}$, $d\vartheta/d\theta \equiv \langle \mathbf{B}\cdot\nabla\theta\rangle/\mathbf{B}\cdot\nabla\theta$, and $\langle\cdots\rangle$ denotes an average over $\vartheta$. The two most important control parameters in Eq (4) are

$$g = -\frac{m_i n_i I}{e\tau_{iz}n_z\langle\mathbf{B}\cdot\nabla\theta\rangle}\left(\frac{d\ln n_i}{d\psi} - \frac{1}{2}\frac{d\ln T_i}{d\psi}\right) = O(\Delta),$$

$$M^2 = M_z^2\left(1 - \frac{zm_i}{m_z}\frac{T_e}{T_e+T_i}\right),$$

which measure the steepness of the plasma profile and the toroidal rotation speed, respectively. The ion-impurity collision time is denoted by $\tau_{iz} = 3(2\pi)^{3/2}\epsilon_0^2 m_i^{1/2}T_i^{3/2}/n_z z^2 e^4\ln\Lambda$. The remaining parameter, $\gamma$, that appears in Eq (4) is of order unity and does not play an important role in the theory.

The impurities are pushed toward the inboard side of the torus when $g$ becomes large, and the neoclassical transport then becomes a strongly nonlinear function of the gradients. On the other hand, when the toroidal rotation is so large that $M \gtrsim 1$, the impurities are pushed to the outside of the torus by the centrifugal force, and this also affects the transport. In a plasma with small inverse aspect ratio, $\epsilon \ll 1$, and circular cross section, Eq (4) can be solved by making the expansions $b^2 = 1 - 2\epsilon\cos\theta + O(\epsilon^2)$, $n = 1 + n_c\cos\theta + n_s\sin\theta + O(\epsilon^2)$, $M^2 = M_0^2(1+2\epsilon\cos\theta) + O(\epsilon^2)$. The classical and neoclassical particle fluxes then become

$$\langle\mathbf{\Gamma}_i\cdot\nabla\psi\rangle = \frac{\epsilon^2 p_z}{q^3 e}\left(1 + \frac{2\Lambda q^2}{1+\left(\frac{1+\gamma}{1+\alpha}\right)^2 g^2}\right)g, \qquad (5)$$

where the first term is the classical flux and the second term, which contains the factor

$$\Lambda = \left(1 + \frac{M_0^2}{1+\alpha}\right)\left(1 + \frac{1+\gamma}{1+\alpha}M_0^2\right), \qquad (6)$$

represents the neoclassical flux. The latter exceeds the former by the Pfirsch-Schlüter factor $2q^2$ when the gradients and the rotation are weak, $g \ll 1$ and $M_0^2 \ll 1$. When either $g$ or $M_0$ is not small, new and potentially important effects emerge.

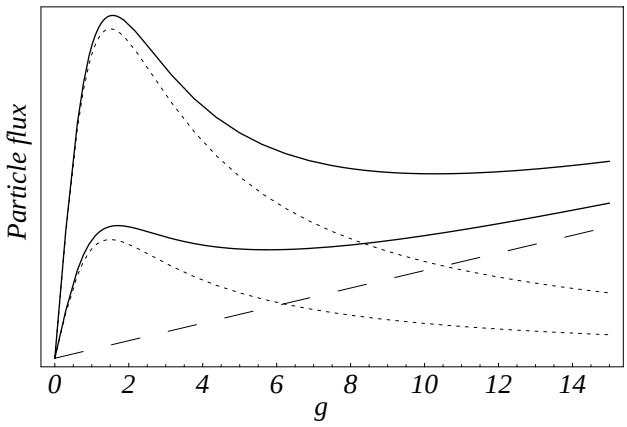


Figure 4: *Ion particle fluxes versus normalized gradient $g$ in a large-aspect-ratio tokamak with circular cross section, $\epsilon \ll 1$, $\alpha = 0.5$. The dashed line is the classical flux, the dotted lines are neoclassical fluxes, and the solid lines represent the sum of classical and neoclassical fluxes. The lower pair of dotted and solid lines are for vanishing toroidal rotation, $M_0^2 = 0$, and the upper pair for impurity Mach number $M_0^2 = 1$.*

First, if the gradients are weak but the rotation is significant, i.e., if $g \ll 1$ and $M_0 = O(1)$, the neoclassical flux is increased by the factor $\Lambda$ in Eq (6) over the usual Pfirsch-Schlüter result. The diffusion coefficient thus becomes $D = (1+2\Lambda q^2)D_{cl}$, where $D_{cl} = T_i/m_i\Omega_i^2\tau_{iz}$ is the classical diffusion coefficient and $2q^2 D_{cl}$ the Pfirsch-Schlüter diffusion coefficient. The enhancement factor $\Lambda$ can be quite large if $M_0$ exceeds unity, as is frequently the case for heavy impurities. The second conclusion to draw from Eq (5) is that if the pressure or temperature gradient becomes sufficiently steep ($g \gg 1$) the neoclassical flux is suppressed since the denominator in the second term of Eq (5) depends quadratically on $g$. Classical transport then dominates, and the total flux is a non-monotonic function of the gradients [8]. Figure 5 shows the particle fluxes as functions of $g$. Conventional transport theory only treats the lower left corner of this figure, where the flux is proportional to the gradient. Note that the total flux (solid lines) depends on the gradients in a way characteristic of bifurcating systems.

We now consider the limit $g \gg 1$, where the neoclassical transport tends to be suppressed. Expanding the solution of Eq (4) in $g^{-1}$ gives

$$n = \frac{\gamma}{\left(1 - \left\langle (1+\gamma b^2)^{-1} \right\rangle\right)} \frac{b^2}{1+\gamma b^2} + O\left(g^{-1}\right),$$

indicating that the impurities are pushed toward the inboard side of the torus. The neoclassical cross-field particle flux now becomes

$$\left\langle \mathbf{\Gamma}^{neo} \cdot \nabla\psi \right\rangle = -\frac{I \left\langle p_z \right\rangle \left\langle \mathbf{B} \cdot \nabla\theta \right\rangle \gamma}{e \left\langle B^2 \right\rangle \left(1 - \left\langle (1+\gamma b^2)^{-1} \right\rangle\right)} \left\langle \frac{\partial M^2/\partial\vartheta}{1+\gamma b^2} \right\rangle.$$

This flux vanishes unless the rotation is finite and the equilibrium is up-down asymmetric. The residual transport, which for instance could occur in a steep edge transport barrier,

has a number of surprising properties. It can be either inward or outward, and it depends on the geometry of the magnetic field in a non-trivial way. For instance, in the particularly simple limit $\gamma \ll 1$, $\epsilon \ll 1$, $n_z z^2 \ll n_i$, the flux becomes

$$\langle \mathbf{\Gamma}^{neo} \cdot \nabla \psi \rangle = 0.33 \frac{f_c I \langle p_z \rangle}{e \langle B^2 \rangle^2 \left( \frac{d \ln n_i}{d \ln T_i} - \frac{1}{2} \right)} \left\langle B^2 \mathbf{B} \cdot \nabla M^2 \right\rangle$$

and is thus independent of the collision frequency although it is caused by Coulomb collisions. Remarkably, it is proportional to $I = RB_\zeta$ and therefore changes sign if the toroidal field is reversed. If the density profile is at least half as steep as the temperature profile, which is normally the case in the tokamak edge, and the magnetic field has a single X-point below the midplane, the flux is inward if $\mathbf{B} \times \nabla B$ is downward, and vice versa. Thus, if the ion $\nabla B$-drift is toward the X-point, which is experimentally favourable for attaining the high-confinement H-mode, the neoclassical bulk-ion particle flux is inward, and the impurities (whose flux is opposite to that of the main ions) are prevented from entering the plasma core.

## 4. Suppression of runaway avalanches by radial diffusion

Runaway electrons are frequently generated in tokamak disruptions. In future, large tokamaks it is thought that close Coulomb collisions between thermal electrons and existing runaways can lead to catastrophic exponential multiplication of the latter – a so-called runaway avalanche. The existing theory of this process [10] assumes that there is no loss of runaway electrons. In practice, these particles undergo radial transport due to magnetic fluctuations and are thus imperfectly confined. We have calculated the reduction of the avalanche growth rate that this causes, both by an analytical approximation and by three-dimensional Monte Carlo simulation of the avalanche kinetics in full toroidal geometry [11].

As a runaway electron is accelerated by the electric field, the diffusion coefficient $D(p)$ decreases progressively with increasing (relativistic) parallel momentum $p = (1 - v^2/c^2)^{-1/2} m_e v_\parallel$. By solving the kinetic equation for diffusing runaway electrons generated by close collisions, we have derived an approximate formula for the avalanche growth rate

$$\gamma = \gamma_r \exp\left( -\frac{\tau (2.4/a)^2}{m_e c (E_\parallel / E_c - 1)} \int_0^\infty D(p) dp \right), \tag{7}$$

where $\gamma_r$ is the growth rate calculated in Ref 10 in the absence of diffusion, $a$ the minor radius, $\tau = 4\pi\epsilon_0^2 m_e^2 c^3 / n_e e^4 \ln\Lambda$ the collision time for relativistic electrons, and $E_c = m_e c / e\tau$ the critical field for runaway production. We have also developed a 3D Monte Carlo code, ARENA, that simulates runaway avalanches in toroidal geometry and includes the effects of collisions, radial diffusion, synchrotron radiation reaction, and a self-consistently induced electric field. The numerically calculated growth rate agrees with the analytical result given here, see Fig 5. Thus, the avalanche growth rate becomes very small when stong radial diffusion is present. As the poloidal magnetic flux that is available to induce an electric field is finite, avalanches are prevented altogether by sufficiently strong radial diffusion. The requisite magnetic fluctuation level is sensitive to the mode structure and the speed of the disruption, and can be estimated to be around $\delta B/B \sim 10^{-3}$ for JET and ITER-like parameters. Thus, it appears possible that the naturally occurring, or any externally induced, magnetic fluctuations could significantly reduce the size of secondary runaway avalanches [12].

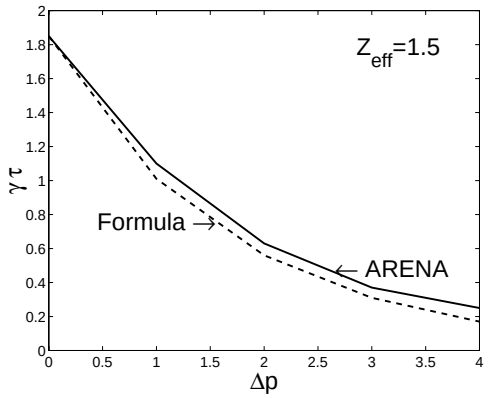


Figure 5: *The normalized growth rate $\gamma\tau$ vs $\Delta p$ for the diffusion coefficient $D(p) = D_0 e^{-(p/m_e c\Delta p)^2}$, with $D_0 = R^2/\tau$, $a/R = 0.31$, and $Z_{\rm eff} = 1.5$. The solid line shows the result from the numerical simulation, and the dotted line the analytical approximation (7).*

## 5. Conclusions

The CUTIE global simulation code has demonstrated how the interaction of turbulence with the evolution of the equilibrium can lead to the spontaneous formation of ITBs near rational surfaces, in qualitative agreement with JET and RTP. When steep gradients form as turbulence is suppressed near the plasma edge residual collisional particle fluxes (appropriately modified for steep gradients) exhibit interesting features: a bifurcation to low fluxes; the direction of the flux is affected by the position of an X-point, so that if the ion-$\nabla B$-drift is towards the X-point impurities are screened from the core; and impurities are redistributed poloidally in a way that should be experimentally detectable. Finally, it has been shown that magnetic turbulence with $\delta B/B \sim 10^{-3}$ can suppress runaway avalanches in large tokamaks.

This work was funded jointly by the UK Dept of Trade and Industry, and Euratom under association contracts with France, Italy, Sweden and the UK.

## References

[1] BELL, M.G., *et al*, Plasma Phys. Control. Fusion **41** (1999) A719.
[2] GORMEZANO, C., Plasma Phys. Control. Fusion **41** (1999) B367.
[3] HOGEWEIJ G.M.D.,*et al*, Nucl. Fusion **38** (1998) 1881.
[4] THYAGARAJA, A., Proc. 27th Euro.Phys. Soc. Conf. Budapest (to appear in Plasma Physics and Contr. Fusion); also, UKAEA Fusion Report, FUS 428 (2000).
[5] HASEGAWA, A. and WAKATANI, M., Phys. Rev. Lett. **59** (1987) 1581.
[6] HINTON, F.L. and ROSENBLUTH, M.N., Plasma Phys. Control. Fusion **41** (1999) A653.
[7] HSU, C.T., and SIGMAR, D.J., Plasma Phys. Control. Fusion **32** (1990) 499.
[8] HELANDER, P., Phys. Plasmas **5** (1998) 3999.
[9] FÜLÖP, T., and HELANDER, P., Phys.Plasmas **6** (1999) 3066.
[10] ROSENBLUTH, M.N., and PUTVINSKI, S.V., Nucl. Fusion **37** (1997) 1355.
[11] HELANDER, P., ERIKSSON, L.-G., and ANDERSSON, F., to appear in Phys. Plasmas **7** October (2000).
[12] YOSHINO, R., TOKUDA, S., and KAWANO, Y., Nucl. Fusion **39** (1999) 151.